BBC RD 1985/11

BBC

RESEARCH DEPARTMENT

REPORT

ROOM MODES and SOUND ABSORPTION: Some practical measurements compared with theoretical predictions

E.W. Taylor, M.A.(Cantab.), C.Eng., M.I.E.E.

Research Department, Engineering Division
THE BRITISH BROADCASTING CORPORATION

August, 1985

ROOM MODES AND SOUND ABSORPTION: SOME PRACTICAL MEASUREMENTS COMPARED WITH THEORETICAL PREDICTIONS

E. W. Taylor, M.A.(Cantab), C.Eng., M.I.E.E.

Summary

Changes in the amount of sound absorption, which occur when absorbing material is placed in turn at different regions of a standing wave (room mode) pattern in a reverberant enclosure, are discussed. Theoretical predictions of this change of absorption are compared with practical measurements. The dependence of the degree of excitation of the absorbing surface on the standing wave pattern over its area, the relative importance of the potential and kinetic energy components in the sound field, and the acceptance of energy from regions of the sound field not immediately adjacent to the absorber, are cited as causes of the observed differences between the theoretical and practical results.

Issued under the Authority of

M. E. B. Maffett

Head of Research Department

Research Department, Engineering Division,
BRITISH BROADCASTING CORPORATION

August 1985

(PH-266)

ROOM MODES AND SOUND ABSORPTION: SOME PRACTICAL MEASUREMENTS COMPARED WITH THEORETICAL PREDICTIONS

E. W. Taylor, M.A.(Cantab.), C.Eng., M.I.E.E.

ROOM MODES AND SOUND ABSORPTION: SOME PRACTICAL MEASUREMENTS COMPARED WITH THEORETICAL PREDICTIONS

E. W. Taylor, M.A.(Cantab.), C.Eng., M.I.E.E.

1. Introduction

The idea of studying the sound decay in a room by considering the decay of individual room modes (standing waves within the room) caused by the presence of absorbing material has been discussed elsewhere.[1] A relationship based on a theoretical treatment of the subject by Dowell[2] leads to the derivation of a "damping coefficient" which is analogous to the more conventional absorption coefficient but takes into account the size and disposition of the patches of absorbing material on the surfaces of the room, and the frequency of excitation and room geometry insofar as these factors influence the formation of room modes. In turn, the damping coefficient value found for particular absorber layout and room mode conditions (e.g. in reverberation room measurements) is used to derive a value of specific acoustic impedance (assumed real in the present work). This impedence value is then used to determine a new value of damping coefficient for the conditions under which the absorbing material will be used in practice, enabling the sound decay of the relevant room mode to be found. A summation of the decays of the room modes falling within (say) a one-third octave frequency band then gives a prediction of the reverberation time of the room into which the absorbing material has been introduced.

The procedure outlined above involves a number of approximations to the conditions which actually occur in practice. A foreseen difficulty, for example, is the assumption that the specific acoustic impedance of the absorbing material is real and invariant: in reality, the impedance is usually complex and depends on the angle of incidence of the sound wave. Tests were therefore planned to examine the degree of accuracy with which this procedure could be used in practice to predict room mode decay times (in a given frequency band) for one set of conditions from measured decay times taken under another set of conditions. In principle the change in acoustic conditions could take a variety of forms: for example, a change in the size and position of the absorbers in use, a change in the size and shape of the room (which would affect the room mode pattern) or a combination of such changes. In order to simplify the experimental procedure it was decided to carry out tests using patches of absorbing material of fixed size and shape, and to examine the effect of placing this material in different places in one test room. Furthermore, only excitation frequencies corresponding to the lowest-order axial room modes were used. It was thought that other test conditions could be introduced at a later stage, once the validity of the theoretical model used for the decay-time predictions had been established. However, these first tests revealed very considerable differences between the practical amounts of sound absorption obtained when an absorber was exposed to different standing wave pattern configurations on the one hand, and the corresponding theoretical prediction of the change of absorption on the other hand. This Report examines these differences in terms of patterns of sound energy flow and possible mechanisms of sound absorption.

2. Relationships between the properties and distribution of absorbing material, the room modes and the sound decay

2.1. General relationships

For convenience, the relationships between the absorbing material and room mode parameters discussed in Reference 1 are re-stated in this Section.

Consider a rectangular room having dimensions L_x, L_y and L_z along the three coordinate axes (Fig. 1). Room modes are characterised by the number of nodal planes (n_x, n_y and n_z) perpendicular respectively to each of the axes. In the present case each such mode will for descriptive convenience be identified by a single symbol (n) where different values of n signify different combinations of the three values, n_x, n_y and n_z. For the n^{th} mode, then, and for a rectangular patch of absorbing material on one or other of the two surfaces of the enclosure normal to the z co-ordinate axis (Fig. 2), an "integration

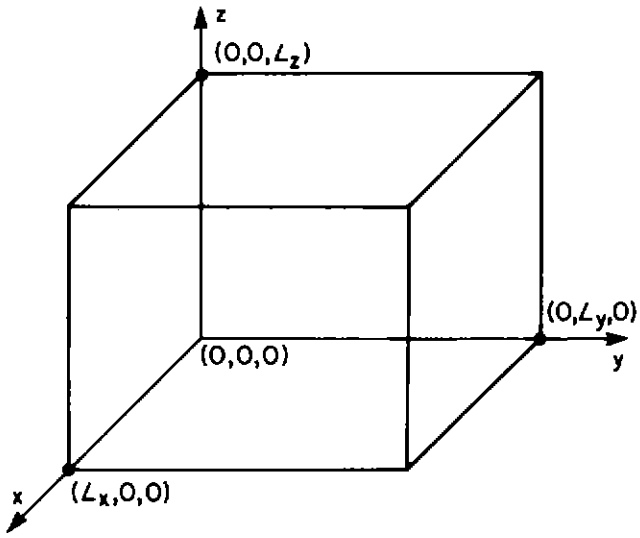

Fig. 1 – Coordinate axes for a room.

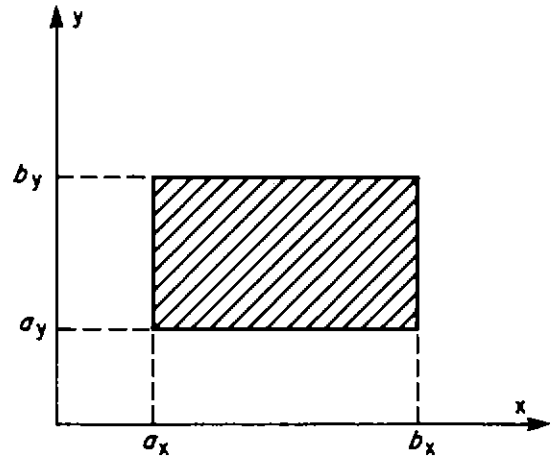

Fig. 2 – Coordinates of patch of absorbing material.

factor" $I_{z[n]}$ may be defined, where

$$I_{z[n]} = I(a_x, b_x, a_y, b_y, n_x, n_y)$$
$$= \frac{1}{4}\left[(b_x - a_x) + \frac{L_x}{2n_x}\left(\sin\frac{2n_x b_x}{L_x} - \sin\frac{2n_x a_x}{L_x}\right)\right]\left[(b_y - a_y) + \frac{L_y}{2n_y}\left(\sin\frac{2n_y b_y}{L_y} - \sin\frac{2n_y a_y}{L_y}\right)\right] \quad (1)$$

This integration factor represents the effective area of the absorbing patch in the presence of the n^{th} room mode. If more than one absorbing patch is present on these two surfaces, an integration factor can be calculated for each such patch. Two other sets of integration factors, $I_{x[n]}$ and $I_{y[n]}$, may also be found: these refer to patches of absorbing material on the pairs of surfaces normal to the x- and y-axes respectively, and therefore involve (y, z) and (x, z) coordinates. These parameters still refer to the same (n^{th}) room made.

If there are p patches of absorbing material altogether, then a further "damping factor" D_n may be defined, such that

$$D_n = \frac{1}{\varepsilon_{n_x}\varepsilon_{n_y}\varepsilon_{n_z}}\left(\sum_{\text{all } p}\frac{I_p}{\zeta_p}\right) \quad (2)$$

In Equation 2, ζ_p is the specific acoustic impedance of the surface of the p^{th} patch of absorbing material ($\zeta = 1$ is the impedance of "free air", or in other words of a plane sound wave propagating in the absence of any obstructions), and I_p is the corresponding integration factor, obtained as discussed above. In Dowell's analysis, the acoustic impedance is assumed to be real. The quantities ε are defined by the relationship

$$\varepsilon_n \begin{cases} = 1 \text{ when } n = 0 \\ = \frac{1}{2} \text{ when } n \geqslant 1 \end{cases} \quad (3)$$

The reverberation time for the n^{th} room mode is then given by

$$T_n = \frac{6V.ln\,10}{cD_n} \quad (4)$$

In Equation 4, V is the volume of the room, c the velocity of sound, and ln 10 is the natural logarithm of 10 (2.3026).

2.2. Relationships for particular absorber and room-mode conditions

In the work discussed in this Report only one "test" patch of absorbing material was used, although other "shielding" patches of material were at times also used to modify the direction of energy flow (see Section 5.4). Furthermore, only the lowest-order axial room modes were excited. These conditions enable considerable simplifications to be made to Equations 1 and 2.

The damping factor relating to the patch of absorbing material may be found by measuring the reverberation time of the enclosure both in the absence and in the presence of the patch of material. The position in the enclosure where the patch is placed is also required. Using subscripts "E" and "F" to denote these conditions respectively and for simplicity omitting other subscripts it can be seen from Equation 4 that

$$T_E = \frac{KV}{D_E} \tag{5}$$

$$\text{and } T_F = \frac{KV}{D_F} \tag{6}$$

$$\text{where } K = \frac{6 \ln 10}{c} \tag{7}$$

From Equations 5 and 6

$$\frac{T_F}{T_E} = \frac{D_E}{D_F} \tag{8}$$

In the same terms the damping factor relationship (Equation 2) may be written

$$D_F = \frac{1}{\varepsilon_x \varepsilon_y \varepsilon_z}\left(\frac{I_A}{\zeta_A} + \frac{I_E}{\zeta_E}\right) \tag{9}$$

where the additional subscript "A" refers to the patch of absorbing material by itself. Furthermore, to a sufficient degree of approximation

$$D_E = \frac{1}{\varepsilon_x \varepsilon_y \varepsilon_z} \cdot \frac{I_E}{\zeta_E} \tag{10}$$

The approximation occurs because the value of the integration factor I_E is strictly speaking not the same in Equations 9 and 10: placing the patch of absorbing material on a surface of the enclosure obscures a corresponding part of the surface itself, thus affecting the value of this factor. In the present case, however, the patch of material has only some 1.5% of the total surface area of the enclosure, and the resulting difference in integration-factor value may be discounted. From Equations 9 and 10, therefore,

$$D_F = D_A + D_E \tag{11}$$

where

$$D_A = \frac{1}{\varepsilon_x \varepsilon_y \varepsilon_z} \cdot \frac{I_A}{\zeta_A} \tag{12}$$

D_A being the damping factor introduced by the patch of absorbing material. From Equations 8 and 11

$$\frac{T_F}{T_E} = \frac{D_E}{D_A + D_E} \tag{13}$$

Hence, from Equations 5 and 13,

$$D_A = KV\left(\frac{1}{T_F} - \frac{1}{T_E}\right) \tag{14}$$

Invoking the approximation involved in deriving Equation 10 permits this simple relationship to be used, rather than the more complicated procedure of calculating the specific acoustic impedance of the walls of the empty enclosure, and then calculating a new damping factor for the empty enclosure which takes account of the smaller wall area exposed when the absorbing patch is present. Knowing the value of D_A, the specific acoustic impedance of the surface can be obtained if required using Equations 7 and 12. In the present work, however, practical measurements and theoretical predictions involving the same excitation frequency (and therefore the same room mode) are compared. Throughout such comparisons the $1/\varepsilon_x\varepsilon_y\varepsilon_z$ factor remains constant, and it is also assumed (see Section 1) that the specific acoustic impedance is invariant (this aspect is discussed in Section 6). Under these conditions it can be seen from Equation 12 that the damping factor is directly proportional to the integration factor, and it is therefore convenient to conduct the discussion in terms of these two quantities, without invoking the actual value of specific acoustic impedance.

When the reverberation time of the empty enclosure is large compared with the value obtained with the absorbing material present, the damping factor relating to the empty enclosure (D_E) may be neglected. The damping factor introduced by the patch of absorbing material then becomes the same as the overall damping factor of the treated room (i.e. $D_A = D_F$ from Equation 11) and can therefore be found directly using Equation 6. This approximation has however not been used in the present work.

Turning now to the simplification of the integration-factor equation (Equation 1), it may first be noted that in the case of the lowest-order axial room modes two of the three quantities n_x, n_y and n_z are zero, the other one being unity. Since $(\sin k\alpha)/\alpha = k$ when $\alpha = 0$ the following simplified relationships can be derived:

$$I_{x[100]} = (b_y - a_y)(b_z - a_z) \tag{15}$$

$$I_{y[100]} = \tfrac{1}{2}(b_z - a_z)\left[(b_x - a_x) + \frac{L_x}{2\pi}\left(\sin\frac{2\pi b_x}{L_x} - \sin\frac{2\pi a_x}{L_x}\right)\right] \tag{16}$$

$$I_{x[010]} = \tfrac{1}{2}(b_z - a_z)\left[(b_y - a_y) + \frac{L_y}{2\pi}\left(\sin\frac{2\pi b_y}{L_y} - \sin\frac{2\pi a_y}{L_y}\right)\right] \tag{17}$$

$$I_{y[010]} = (b_x - a_x)(b_z - a_z) \tag{18}$$

The subscript convention used in Equations 15–18 has been discussed in relation to Equation 1. Similar relationships can of course be derived for other room modes, but these are not required in discussing the present work.

3. Implications of the form of the integration relationship shown in section 2.1.

3.1. Energy density of the sound field in a tube

Consider a standing wave in a tube of length l, of such dimensions that plane wave fronts propagate through the tube. The air in the tube is excited by a piston in the tube at coordinate $x = 0$ and terminated by a rigid end-plate at coordinate $x = l$. In general, the instantaneous sound pressure $p(x, t)$ at a distance x from the piston is given[3] by

$$p(x, t) = \sqrt{2}\rho_o c|u_o|\frac{\sin\omega t \cos k(l - x)}{\sin kl} \tag{19}$$

while the instantaneous particle velocity $u(x, t)$ is given by

$$u(x, t) = \sqrt{2}|u_o|\frac{\cos\omega t \sin k(l - x)}{\sin kl} \tag{20}$$

In Equations 19 and 20, ρ_o and c are the density of air and the velocity of sound in it, u_o is the rms velocity of the piston (and therefore the air immediately in front of it), ω is the angular frequency of the piston, and k is the wave-number ($k = 2\pi/\lambda = \omega/c$ where λ is the wavelength).

In general, the absorption of sound at a surface depends on the sound power available at the surface. The sound power is proportional to the energy density of the sound field in the room containing the surface: thus, for example, doubling the power of the sound source in the room will double the energy density and in turn double the amount of power absorbed. When the energy density in a room is non-uniform, the amount of power absorbed will depend on the "effective" energy density in the part of the sound field in which the absorber is placed. The total energy density in a sound field can be divided into two components: potential energy density due to sound pressure (i.e. the mean square distance between air molecules) and kinetic energy density due to the mean square velocity of the air molecules. From Equation 19, the potential energy density $\Delta_p(x, t)$ is given by*

$$\begin{aligned}\Delta_p(x,t) &= \tfrac{1}{2}\frac{(p(x,t))^2}{\rho_o c^2} \\ &= \frac{1}{2\rho_o c^2}\left[\sqrt{2}\rho_o c|u_o|\frac{\sin\omega t\cos k(l-x)}{\sin kl}\right]^2 \\ &= \frac{\rho_o {u_o}^2}{2}\left[\frac{1+\cos 2k(l-x)-\cos 2\omega t-\cos 2\omega t\cos 2k(l-x)}{1-\cos 2kl}\right]\end{aligned} \tag{21}$$

The fact that the denominator in Equation 21 becomes zero when $kl = n\pi$, with the value of Δ_p becoming infinite, merely indicates that the air in the tube resonates when its length is an integral number of half-wavelengths and that the expression contains no term which represents sound absorption within the tube. In practice the potential energy density would reach a high but finite value under these conditions, and it is valid to retain this term in the ensuing discussion, even though the expressions so derived will be applied to conditions (the existence of room modes) which involve air resonance.

Equation 21 may be written

$$\Delta_p(x,t) = F[1 + (2\cos^2 k(l-x) - 1) - (2\cos^2\omega t - 1) - (2\cos^2\omega t - 1)(2\cos^2 k(l-x) - 1)] \tag{22}$$

where

$$F = \frac{\rho_o {u_o}^2}{2(1-\cos 2kl)} \tag{23}$$

Remembering that the average value of $\sin^2 a$ or $\cos^2 a$ is $\frac{1}{2}$ (a being a general variable), the time-average value of potential energy density ($\Delta_p(x)$) is given by

$$\begin{aligned}\Delta_p(x) &= F\,.\,2\cos^2 k(l-x) \\ &= F[1+\cos 2k(l-x)]\end{aligned} \tag{24}$$

At the tube termination, $(l - x) = 0$ and hence the time-average potential energy density immediately in front of the termination is $2F$. The potential energy density normalised with reference to the value in this position ($\Delta_{pn}(x)$) is therefore given by

$$\Delta_{pn}(x) = \tfrac{1}{2}[1 + \cos 2k(l-x)] \tag{25}$$

*The symbol Δ is used for energy density, instead of the more usual symbol D: this is reserved for representing the damping factor defined in Equation 2.

The kinetic energy density $\Delta_k(x, t)$ is given by

$$\begin{aligned}\Delta_k(x,t) &= \tfrac{1}{2}\rho_o(u(x,t))^2 \\ &= \frac{\rho_o}{2}\left[\sqrt{2}|u_o|\frac{\cos\omega t \sin k(l-x)}{\sin kl}\right]^2 \\ &= \frac{\rho_o u_o^2}{2}\left[\frac{1-\cos 2k(l-x)+\cos 2\omega t-\cos 2\omega t\cos 2k(l-x)}{1-\cos 2kl}\right]\end{aligned} \tag{26}$$

Using the same treatment as adopted in discussing potential energy density, Equation 26 may be written

$$\Delta_k(x,t) = F[1-(1-2\sin^2 k(l-x))+(1-2\sin^2\omega t)-(1-2\sin^2\omega t)(1-2\sin^2 k(l-x))]$$

The time average value of kinetic energy density ($\Delta_k(x)$) is then given by

$$\begin{aligned}\Delta_k(x) &= F\,.\,2\sin^2 k(l-x) \\ &= F[1-\cos 2k(l-x)]\end{aligned} \tag{27}$$

and using the same factor as in the case of potential energy density (i.e. in terms of the time average potential energy immediately in front of the termination) the normalised time average kinetic energy density becomes

$$\Delta_{kn}(x) = \tfrac{1}{2}[1-\cos 2k(l-x)] \tag{28}$$

From Equations 25 and 28 it can be seen that the total time average energy density along the tube is independent of position.

3.2. Energy density in an enclosure, in the presence of an axial room mode

The expressions for normalised potential and kinetic energy density (Equations 25 and 28) may now be adapted to represent the case of a rectangular room in which a single axial mode is excited. In such a mode, plane waves travel normally between two opposite walls. Consider propagation along the x-axis of the room, the distance between the two reflecting walls being L_x (Fig. 1). Thus l in Equations 25 and 28 may be replaced by L_x. Room modes will exist when the distance between the reflecting walls is an integral number (n) half-wavelengths, that is

$$L_x = n\frac{\lambda}{2} \quad \text{or} \quad \lambda = \frac{2L_x}{n} \tag{29}$$

The integer n is in fact the number of pressure nodes in the standing wave, and is thus the number by which the room mode is characterised.[1] Furthermore,

$$k = \frac{2\pi}{\lambda} = \frac{\pi n}{L_x}$$

Thus Equation 25 becomes

$$\Delta_{pn}(x) = \tfrac{1}{2}\left[1+\cos\frac{2\pi n}{L_x}(L_x-x)\right]$$

The cosine term may be expanded to give

$$\Delta_{pn}(x) = \tfrac{1}{2}\left[1+\cos 2\pi n\,.\,\frac{x}{L_x}\right] \tag{30}$$

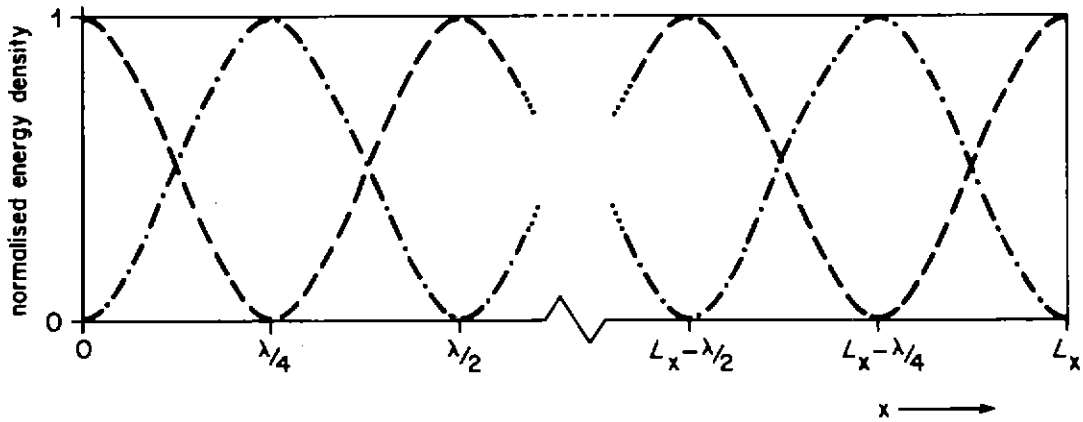

Fig. 3 – Energy density distribution along line parallel to x-axis of room, when excited into axial mode involving reflection at walls perpendicular to this axis.
– – – – – – Potential energy density.
– · – · – · – Kinetic energy density.
——— Total energy density.

This result is an expression of the fact that the room mode is symmetrical with respect to the room, so that it is immaterial which of the pair of reflecting walls contains the origin of coordinates. In a similar manner the relationship involving kinetic energy density (Equation 28) becomes

$$\Delta_{kn}(x) = \tfrac{1}{2}\left[1 - \cos 2\pi n \,.\, \frac{x}{L_x}\right] \tag{31}$$

The distribution of normalised time average potential and kinetic energy density along lines parallel to the x-axis of the room is shown in Fig. 3. Over planes normal to the x-axis the energy density remains constant at a value determined by the distance of the plane from the wall containing the origin of coordinates (or indeed the opposite wall: see the discussion following Equation 30). In particular, the distribution over room surfaces containing the x-direction (the ones not involved in reflecting the travelling waves which together make up the standing wave pattern) conforms to that of Fig. 3 in the x-direction and is uniform in the orthogonal direction.

3.3. Relation between energy density and sound absorption

The absorption of sound by material on the surface of an enclosure will depend on the distribution of energy density in the vicinity of this material. The meaning of the term "vicinity" will be discussed later in this Report, as will the type of energy density (potential or kinetic) to be considered. For the present, however, assume that only potential energy density is effective in causing sound absorption, and that the absorption of sound over a small area of the surface is proportional to the magnitude of the energy density at that area. Absorbers for which this latter assumption is appropriate are said to be "locally reacting". Furthermore, assume that the absorber is in the form of a rectangular patch (see Fig. 2). The energy absorbed (E_{abs}) is then proportional to the integral under the potential energy density curve between limits given by the x-coordinates of the absorber edges (the shaded area in Fig. 4). Thus, from Equation 30,

$$\begin{aligned} E_{abs} &= A\int_{a_x}^{b_x} \Delta_{pn}(x)\mathrm{d}x \\ &= A\int_{a_x}^{b_x}\left(1 + \cos 2\pi n \,.\, \frac{x}{L_x}\right)\mathrm{d}x \\ &= \frac{A}{2}\left[[x]_{a_x}^{b_x} + \left[\frac{L_x}{2\pi n}\sin 2\pi n \,.\, \frac{x}{L_x}\right]_{a_x}^{b_x}\right] \\ &= \frac{A}{2}\left[(b_x - a_x) + \frac{L_x}{2\pi n}\left(\sin 2\pi n \,.\, \frac{b_x}{L_x} - \sin 2\pi n \,.\, \frac{a_x}{L_x}\right)\right] \end{aligned} \tag{32}$$

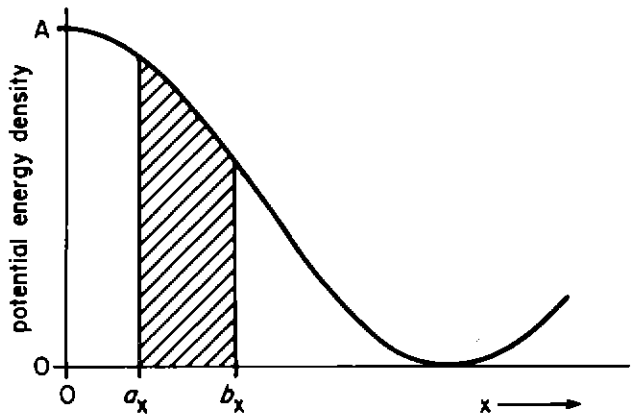

Fig. 4 – Relationship between absorbed energy and potential energy density.
a_x, b_x – Coordinates of absorber edges.
——— *Potential energy density*
▨ *Area proportional to absorbed energy.*

In Equation 32 A is a constant including such items as the normalisation factor involved in deriving Equation 30 (see the remarks following Equation 21) and the length of the absorbing patch in the direction orthogonal to the x-axis (i.e. the value of a_y and b_y in the present case). The point of interest is that the term in square brackets in Equation 32 is the same as the first square-bracketed term in Equation 1. This implies that the relationship derived by Dowell[2] from the theoretical study of sound decay in an enclosure, in which each room mode is treated as a harmonic oscillator damped by the finite wall impedance, involves the assumptions that only potential energy density (not kinetic) is effective in causing sound absorption, and that the absorber is locally reacting. The second square-bracketed term in Equation 1 can similarly be arrived at by considering standing waves set up between the room surfaces normal to the y-axis: the complete Equation 1 is then relevant when the distribution of potential energy density across the surface carrying the absorbing patch is of the "raised cosine" form in both the x- and y- directions, as would be the case for oblique room modes and certain classes of tangential mode.[1a]

If only kinetic energy density was responsible for causing sound absorption, then considerations similar to those used in deriving Equation 32 lead to an integration factor relationship identical to that shown by Equation 1 except that in each square bracket the second complete bracketed term is subtracted from the first bracketed term instead of being added to it. In practice this would have the effect of interchanging the positions at which an absorbing patch would be most and least effective in providing sound absorption. Thus a patch placed symmetrically at a position corresponding to a sound pressure node would give the lowest possible absorption if potential energy provides the mechanism for sound absorption, but the highest possible absorption of kinetic energy density is relevant. This aspect is discussed in Section 5.5.

4. Experimental arrangements

4.1. The test enclosure

All the experiments described in this Report were conducted* in the enclosure originally designed as a "model reverberation room"[4] for use in conjunction with acoustic scaling tests. This was constructed as an open "tank" of 13 mm steel plate, the lid being of 13 mm acrylic sheet. Dimensions are given in Table 1: the coordinate axes refer to Fig. 1. The walls and lid of the enclosure were pierced with a number of access holes, and with one exception (see below) these were sealed either with blanking plates or with modelling clay in the present tests. Apart from samples introduced into the enclosure, it was completely empty: no diffusers were used, and sound excitation was by way of the one unblocked hole, which was near the corner designated as the "origin of coordinates", and to which a loudspeaker high-frequency unit was sealed (on the outside of the enclosure) with an annulus of modelling clay.

* The author wishes to acknowledge the valuable assistance of P.H.C. Legate in carrying out these experiments.

Dimensions	Value
L_x	0.67 m
L_y	0.82 m
L_z	0·71 m
Surface area	3.21 m^2
Volume	0.39 m^3

Table 1 : Dimensions of enclosure used in tests

These precautions were taken to ensure that the lowest possible absorption was achieved in the empty enclosure. Initial tests showed that the principal source of residual absorption was the lid of acrylic sheet. This was hinged along one edge and pulled down onto a resiliant seal by clamps attached to the other three of its edges. Even so, it was found that the amount of absorption introduced by the lid differed from measurement to measurement. It was suspected that a change in clamp tension each time the lid was opened was responsible: this would for example alter the properties of the seal material and therefore its effectiveness in introducing acoustic loss, as well as perhaps changing the modal vibration pattern of the lid itself. The lid was therefore loaded using six 28-lb (12.7 kg) weights (studio scenery weights), each weight resting on three studs fixed to the surface of the lid in order to obtain as consistent a loading pattern as possible. With this technique reasonably consistent "empty" reverberation times could be obtained for the lowest-order modes involving reflection from the (y, z)- and (x, z)-plane walls (the (100) and (010) modes respectively occurring at 257 Hz and 208 Hz). In these cases reverberation times of the order of six seconds were obtained, implying that the mean absorption coefficient for the walls of the enclosure was about 0.003.

In the case of the (001) mode, involving reflections from the (x, y) plane surfaces and therefore the lid of the enclosure, a very much shorter reverberation time than discussed above (of the order of 1.5 seconds) was observed. Indeed, as the frequencies of the (001) and (100) modes are close together (243 and 257 Hz respectively) it was difficult to observe the decay corresponding to the (001) mode, as measurements tended to be obscured by the much greater amplitude (100) resonance. (In this respect the use of filters narrower than the third-octave set used in the present experiments would have been helpful). The reasons for this pronounced dependence of "empty" reverberation time on room mode structure are discussed in Section 5.1.

The technique of loading the lid with weights, in order to reduce sound absorption in the test enclosure and improve the consistency of empty reverberation time measurement, only appeared to be successful in the presence of the (100) and (010) room modes. For higher orders of axial mode, and for all tangential and oblique modes, "empty" reverberation times were obtained which were more in line with the result obtained for the (001) mode mentioned above. The probable explanation for this is that at the higher frequencies involved the vibrational pattern of the lid becomes more complex and less controlled by the presence of the loading weights. For future work to be successful it will be necessary to eliminate this cause of excessive (and inconsistent) loss by constructing the lid of the enclosure of similar material to that used for the walls and base. Some form of seal will however still be required, as a potent source of loss is the presence of a thin crack in a structure, such as inevitably surrounds a lid in the absence of a seal (see Section 5.5).

Fig. 5 shows a general view of the test enclosure and equipment arrangement: the method of loading the lid of the enclosure can be clearly seen.

4.2. Test absorbers

The appraisal of the "damping coefficient" method of determining the reverberation time in an enclosure, as a function of both of the size and disposition of the patches of sound absorbing material

Fig. 5 – General view of test enclosure and equipment.

and also of the intrinsic sound absorbing properties of the material,[2] involves a comparison between the theoretical reverberation-time values obtained by the method outlined in Sections 1 and 2 and practical values measured in the test enclosure. A number of factors in the design and behaviour of the test absorbers used in the practical work are involved in determining whether these two sets of values are, or are not, in agreement. It is therefore important to eliminate as far as possible any known sources of discrepancy, by appropriate design of the test absorbers: it is also important to design these absorbers so that the tests become as sensitive as possible, involving changes in reverberation time which are large compared with the random errors typical of this work.

The principal absorber characteristics which have been considered in the present work are as follows:

(a) Type of material used as the absorbing medium,
(b) Dimensions of the absorbers,
(c) Method of construction of the absorber, and of mounting it on the wall of the enclosure.

As far as the type of material is concerned, it must be locally reacting so that it corresponds with the assumptions made in deriving the basic equations used for reverberation-time prediction (see Section 3). A porous material in which absorption occurs because of the passage of sound through small channels is most suitable; the test absorbers were constructed of "high density" mineral wool (150 kg m^{-3}), which meets this requirement. This material also has the advantage of being in the form of a self-supporting slab, and a framework for containing the material is not required: panel resonances in such a structure could represent a mechanism of sound absorption that is not locally reacting (see Section 5.1). The edges of the slab of material were in fact covered with thick adhesive tape to confer greater rigidity to the absorber and to prevent absorption at these surfaces.

In order to explore the variation of absorption with position relative to the standing-wave mode pattern within the enclosure the dimensions of the absorber should be small compared with this pattern (i.e. compared with a half-wavelength at the frequency concerned). At the same time, the total amount of absorption should, as previously noted, be reasonably high so that changes in reverberation time caused by differing amounts of sound absorption are large compared with random measuring errors. These conflicting requirements are resolved in the present case by constructing the absorber in the form of a long thin rectangular slab of material (707 mm long, 67 mm wide and 31 mm thick). As room excitation by a single axial mode is involved in the present tests, the absorbers can be placed in relation

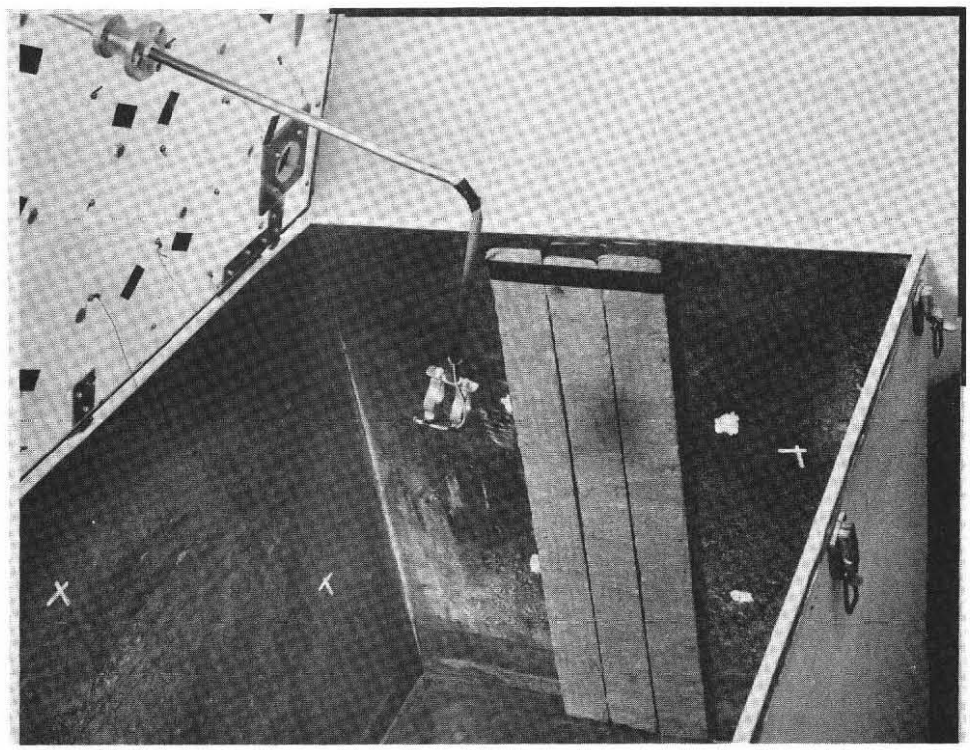

Fig. 6 – Interior of test enclosure, showing test absorbers in position.

to this mode so that its long axis is normal to the direction of sound propagation in the enclosure, while its short axis lies along this direction. The long axis will then lie along a contour of equal sound pressure on the wall to which it is attached, while the short axis will lie in a direction in which sound pressure (or energy density) varies with distance. The fact that the absorber dimension is small in this latter direction, compared with a half wavelength at the excitation frequency, enables the relationship between the amount of absorption and the position of the absorber relative to the standing-wave pattern to be studied in detail. By turning the absorber through a right-angle, so that the long axis lies along the direction of sound propagation, the effect of exposing the absorber to a large fraction of the standing-wave pattern can also be examined. Furthermore, by choosing a different mode of room excitation (or by placing the absorbers on a different wall of the room) so that both the long and short axes are normal to the direction of sound propagation, the effect of a uniform distribution of sound pressure over the surface of the absorber may be included.

The absorbers were attached to the surfaces of the test enclosure with strips of adhesive tape at each end of their long dimension. It has been noted previously (Section 4.1) that thin cracks or gaps in a rigid surface can give rise to sound absorption. In the present case the existence of a gap between the back of the absorber and the surface to which it was attached was found to affect the total absorption in the enclosure considerably. This condition was controlled by sealing the absorber to the surface using adhesive tape applied along the full length of each side of the absorber. The way in which sound absorption changed on sealing this gap gave an insight into the mechanisms of sound absorption existing in different parts of the mode standing-wave pattern: this is discussed in Section 5.5.

Fig. 6 shows a group of three test absorbers attached to a wall of the test enclosure. The use of this absorber configuration is discussed in Section 5.4.

4.3. Measurement equipment

Sound decay in the test enclosure was measured in two ways. In the first place, conventional reverberation-time measuring equipment, in which the gradient of the sound decay (on a logarithmic scale) as displayed on a long-persistence cathode-ray tube is measured with a cursor of adjustable angle, was used. The test enclosure was excited with tone derived from a stable oscillator, the frequency of which could be accurately measured: this enabled particular room modes to be identified unambiguously. Sound was introduced into the enclosure using a small external loudspeaker as described in

Section 4.1, and picked up using a miniature microphone mounted on the end of a rotatable arm passing through the lid of the enclosure. This can be seen in the upper part of Fig. 6. Third-octave filtering was applied to the output signal in order to improve the signal-to-noise ratio of the displayed sound decay. Before measuring reverberation time the oscillator frequency was adjusted about the nominal value for maximum excitation of the test enclosure: this procedure accommodated small changes in resonant frequency, due for example to temperature changes, which could have a significant effect on excitation level because of the very low resonant-cavity damping involved. Following this procedure the sound excitation was pulsed and the reverberation time measured. The value of reverberation time was, as expected, independent of microphone position in the cavity: however, care had to be taken not to place the microphone near a pressure node for the particular room mode concerned, and thereby obtain a low output signal.

Because the two room modes used in the present series of tests were well separated in frequency, it was also possible to derive values of reverberation time from measurements of the figure-of-merit or "Q" of the room-mode resonance. Since

$$\frac{p_t}{p_0} = e^{-\pi f t/Q}$$

where p_t is the sound pressure at time t, p_0 is the sound pressure at $t = 0$ and f is the resonance frequency, and since by definition

$$\frac{p_T}{p_0} = 10^{-3}$$

where p_T is the sound pressure after a time interval equal to the reverberation time T, it follows that:

$$\frac{-\pi f T}{Q} = \ln(10^{-3}) = -6.91$$

or

$$T = \frac{2.20}{f}$$

Furthermore,

$$Q = \frac{f}{\delta f}$$

where δf is the bandwidth of the resonance at its 3dB points. Hence

$$T = \frac{2.2}{\delta f} \tag{33}$$

Reverberation times derived in this way were found to be in good agreement with those measured using the conventional equipment. It may however be noted that the value of δf must be measured with some precision: values of the order of 0.5 Hz were involved, implying a measurement reliability requirement of, say, ± 0.01 Hz.

5. Implications of experimental results on mechanisms of sound absorption

5.1. Absorption associated with the lid of the test enclosure

It has been noted in Section 4 that when measurements of reverberation time in the "empty" test enclosure were made, the reverberation time obtained when the (001) vibrational mode was excited was about one-quarter of the reverberation times measured when the (100) and (010) modes were present. Although not a part of the programme of tests discussed in Sections 5.2–5.5, in which different

configurations of test absorber were introduced and the influence of room mode structure then examined, this effect in itself illustrates a condition where reverberation time is strongly dependent upon room mode structure, and it is therefore interesting to examine the factors underlying this effect.

According to the theory outlined in Section 2, the effective absorption of a surface changes by a factor of two as the sound pressure distribution across it changes from being uniform to having a "raised cosine" characteristic along one dimension.[1a] This behaviour does however depend on the material being "locally reacting", so that absorption at one small area on the surface occurs independently of absorption at other places on the same surface. In the case of the (001) mode, the reverberation time associated with it was very much shorter than this change in effective absorption would imply. Indeed, since in the case of all axial modes two pairs of surfaces are subject to a raised cosine form of sound pressure distribution and one pair to a uniform distribution, this factor by itself would not be expected to give rise to any large difference in reverberation time between the (001) mode on the one hand and the (100) and (010) modes on the other hand, particularly as the enclosure does not depart in a very extreme way from being cubic in form.

An explanation for the very much reduced reverberation time associated with the (001) mode, or in other words for the enhanced sound absorption associated with this mode, appears to lie in the different amount of acoustic coupling between the lid of the enclosure and the sound field inside it when this mode is excited, compared with the coupling existing for the (100) and (010) modes. Measurements using an accelerometer placed at various positions on the lid showed that with equal energy density in the sound field within the enclosure in the two cases, the magnitude of vibration of the lid was on average five times as great when the (001) mode was excited, relative to the presence of the (100) mode. Indeed, at the centre of the lid, no vibration could be detected in the presence of the (100) mode while a significant amount was present using the (001) mode. Assuming that the absorption due to lid vibration is proportional to the amplitude of this vibration, and regarding the Sabine reverberation-time formula as applicable so that reverberation-time is inversely proportional to absorption coefficient, the observed average ratio of lid vibration magnitude for the (001) and (100) modes is consistent with the observed changes in reverberation time in the two cases. The difference in acoustic coupling in the two instances may be explained by assuming that the lid of the enclosure tends to vibrate in a "piston-like" manner with uniform motion over its whole surface. In the case of the (001) mode all portions of the surface will be excited in phase and will therefore sum to give the final amount of excitation. When the (100) mode is present a pressure node is present along a line through the centre of the plate parallel to the y-axis (see Fig. 8, Section 5.2). The sound pressure on one side of this line is in antiphase to the sound pressure on the other side: consequently the two components cancel and the overall excitation of the lid of the enclosure is in principle zero. In practice this cancellation is incomplete, the partial cancellation which does occur being responsible for the effects described above. A similar argument can be applied involving the (010) mode rather than the (100) mode: here the only difference is that the pressure nodal line across the surface of the lid would be parallel to the x-axis rather than the y-axis.

In the foregoing discussion it is implicit that the absorption due to the lid of the enclosure is due to movement of the lid as a whole, in the process of which some acoustic loss is incurred. No attempt has been made to trace the cause of this loss: most likely it is produced by acoustic coupling to the rather "lossy" foam material used as a compression seal round the edges of the enclosure. Because of the lower surface density of the lid (acrylic sheet) as compared with the rest of the structure (heavy steel sheet) the vibration magnitude of the lid will be correspondingly greater: thus greater coupling is to be expected from the sound field in the enclosure to the lossy sealing material by way of the lid, rather than by way of the walls of the enclosure (which are of course also in contact with the sealing material).

The influence of the relatively lightweight lid of the enclosure on the achievable "empty" reverberation times, as a function of room mode structure, is not predicted by the theoretical work outlined in Sections 2 and 3, since this work assumes the absorbing material to be locally reacting (see Section 6). Nevertheless, panel absorbers are often used for acoustic treatment (for example, wood panelling is used for control of low-frequency reverberation time) and the considerations discussed above are of direct relevance in such cases.

5.2. Tests using single absorbing patches in the enclosure

An absorbing patch, of the type described in Section 4.2, was placed in turn at each of the four positions within the test enclosure shown in Fig. 7, and itemized in Table 2. Reverberation-time measurements were made in each case with excitation frequencies corresponding to the (100) and (010) room modes. The reason for not using the (001) mode as well has been discussed in Section 5.1. In addition, reverberation-time measurements were made with the enclosure empty. Table 3 shows the values obtained. At least two completely independent measurements were made using each test condition, the absorbing patch being removed and replaced in position between the measurements. It was found that on average the individual reverberation-time measurements were consistent to within $\pm 8\%$ of the mean values obtained.

Table 3 shows these mean values, and in addition the corresponding values of damping coefficient calculated using Equation 14 (Section 2.2). It may first be noted that the damping factor varies by a factor of about three in the case of excitation of both the (100) and (010) room modes, depending on the position in which the absorbing patch was placed in the test enclosure. Since damping factor and

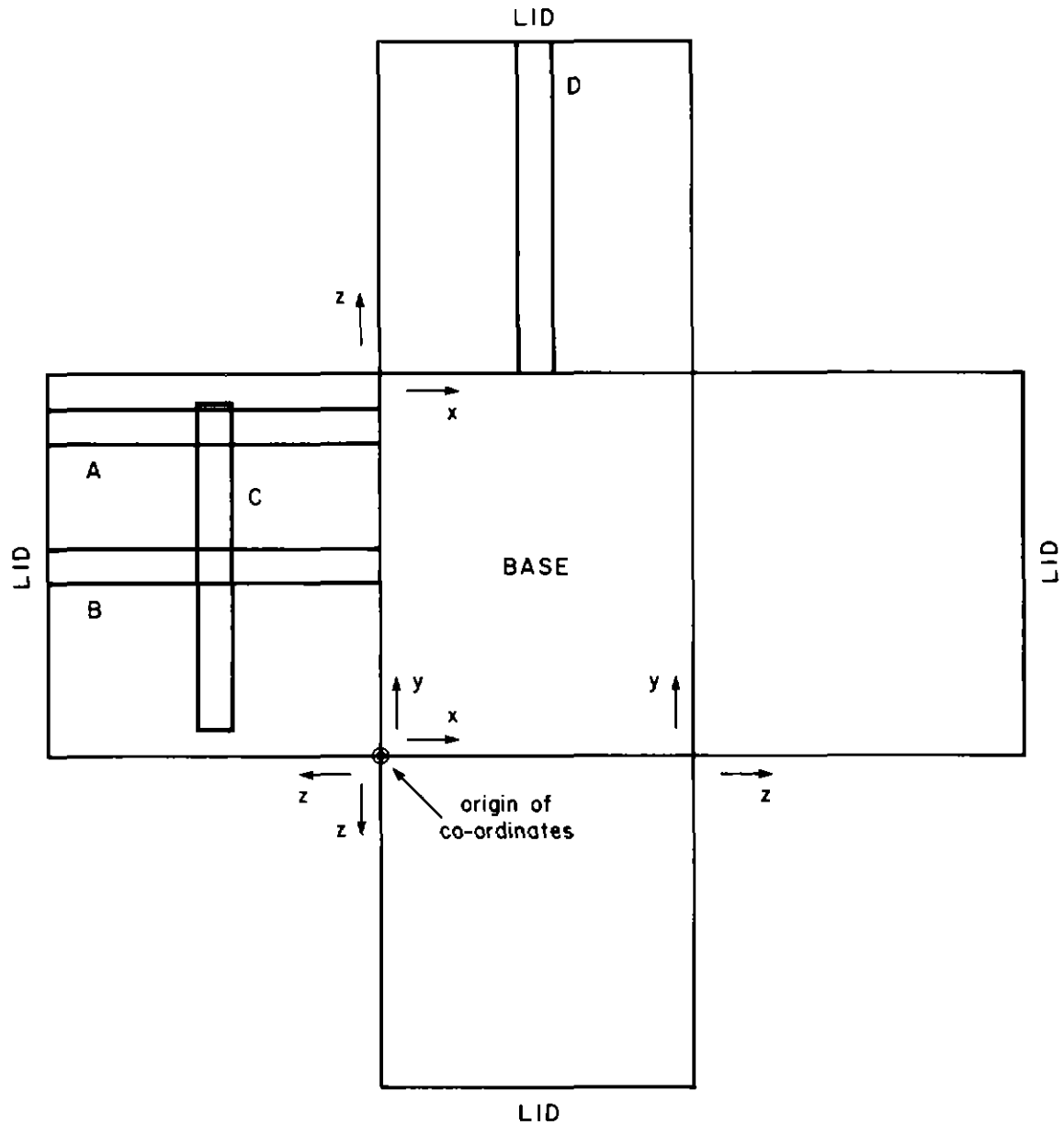

Fig. 7 – "Unfolded" diagram of test enclosure, showing absorbing patch positions. See Table 2 for dimensions.

Condition Reference	Position of absorbing patch		
	Axis normal to surface to which patch is attached	Position of centre-line of patch	
		Long dimension	Short dimension
A	x	vertical 100.5 mm from edge of enclosure	horizontal along centre-line of surface
B	x	vertical along centre-line of surface	horizontal along centre-line of surface
C	x	horizontal along centre-line of surface	vertical along centre-line of surface
D	y	vertical along centre-line of surface	horizontal along centre-line of surface

Table 2 : Details of absorbing patch positions in test enclosure

conventional "absorption coefficient" are directly connected by the relationship[1b]

$$S\bar{\alpha} = 4D \tag{34}$$

where S is the area of absorber having absorption coefficient $\bar{\alpha}$ and D is the corresponding damping factor, it can be seen that the measured absorption coefficient would also be subject to a change by a factor of three, depending only on the position of the absorbing patch in the enclosure. Fig. 8 shows the positions of the absorbing patch in relation to the mean square sound pressure (or potential sound energy density as given by Equation 21), for each condition of enclosure excitation. It can be seen that position B corresponds to a position of minimum potential energy density in the ambient sound field when the (010) room mode is excited, and that position D has the same correspondence for the (100) room mode. Values of damping coefficient occurring under these conditions are shown in heavy type in Table 3. It can be seen that the value of damping coefficient is at a minimum under these conditions. In qualitative terms this behaviour is consistent with the amount of absorption that takes place at an absorbing surface depending on the potential sound energy density at the surface of the absorbing patch. In the case of the (010) mode, in fact the "rank order" of the damping coefficient values agrees

Absorbing patch position (see Table 2)	Measured reverberation time for indicated room mode (sec)		Value* of practical damping factor for indicated room mode	
	(100)	(010)	(100)	(010)
A	2.09	2.74	5.00	2.99
B	2.18	4.03	4.69	**1.17**
C	2.71	3.83	3.29	1.37
D	3.81	2.50	**1.64**	3.53
Enclosure empty	6.35	5.78		

Table 3 : Measured reverberation times and practical damping factors using one absorbing patch sealed to walls of test enclosure

*multiply indicated values by 10^{-3}

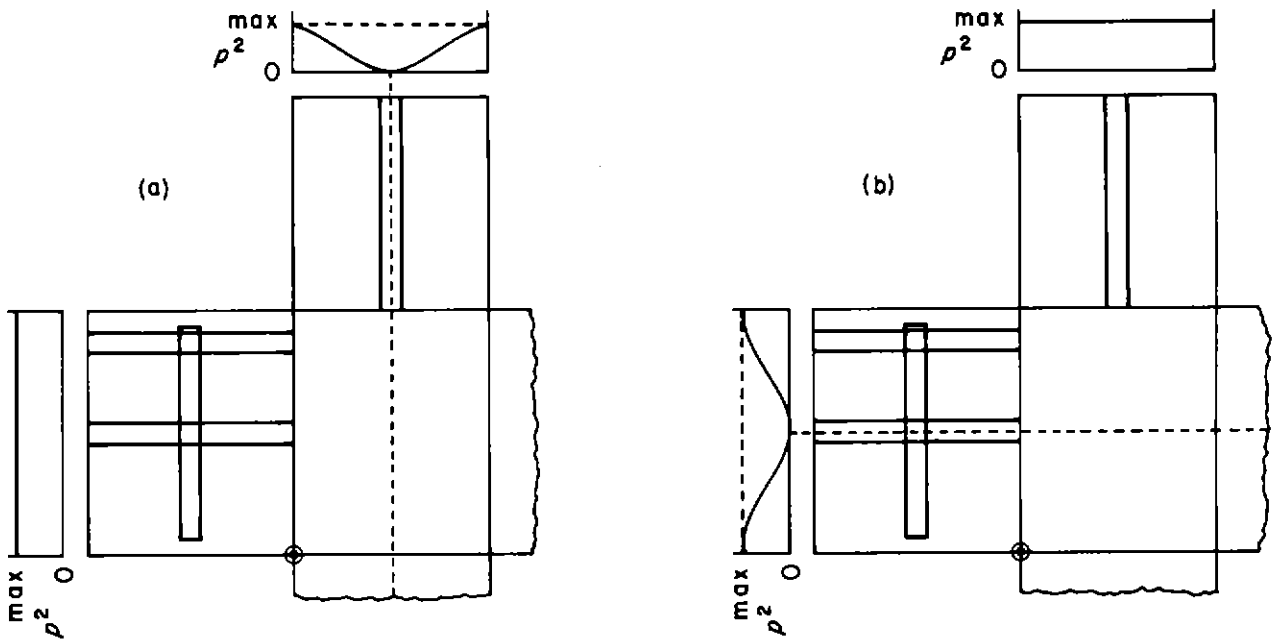

Fig. 8 – Positions of potential sound energy density minima in relation to absorbing patch.
(a) (100) mode.
(b) (010) mode.
---- Potential sound energy density minimum.
⊕ Origin of coordinates (see fig. 7).

with predictions made on this basis. The values of damping coefficient obtained in the case of the (100) mode, on the other hand, show some anomalies in this respect, in that different coefficients are obtained with the patch in positions A, B and C although the potential sound energy density at the surface of the absorber is the same in these three cases. These anomalies are discussed in Section 5.5.

The relationships between the absorbing material and the room mode parameters outlined in section 1 may in principle be used to calculate "theoretical" damping factors. Calculation of such factors in absolute terms requires a knowledge of the specific acoustic impedance of the surface of the material, but damping factor ratios relating to a patch of material placed in turn at different positions in an enclosure, with the excitation frequency held constant so that the same mode is present, may be obtained on the assumption that this impedance is independent of the position of the patch. In fact, a damping factor ratio is simply the ratio of the two corresponding integration factors (Equation 1) relating to the two positions of the patch of material, since the terms in ε in Equation 2 are the same in the two cases (because the same mode is involved) as well as the impedance remaining the same. Table 4 shows such theoretical ratios of damping factor for absorbing material placed in positions B and D of Table 2 and Fig. 7. For both the (100) and (010) modes maximum sound pressure occurs at one of these positions (taken as the numerator in the ratio) and minimum sound pressure at the other (taken as the denominator). Table 4 also shows the corresponding ratios obtained for practical damping factors (see Table 3). It is immediately apparent that the theoretical damping factor ratio is greater, by a large factor (see right-hand column of Table 4), than the practical damping factor ratio, indicating that the assumptions on which the theoretical calculations are based are not justified. Possible reasons for this lack of agreement between theory and practice are examined in the following sections of this Report.

5.3. The effective dimensions of an absorbing patch

It is well known that in the case of a resonant absorber (e.g. a Helmholtz resonator) the effective area of the absorber is many times the actual area of the resonator itself. A. B. Wood[4] shows that this area (S_{eff}) is given by

$$S_{eff} = \lambda^2/4\pi \tag{35}$$

Mode	Absorbing patch positions used in obtaining ratio values	Damping factor ratios for conditions shown in Columns 1 and 2		Factor by which theoretical ratio exceeds practical ratio
		Theoretical (from Equation 1)	From practical results (Table 3)	
(100)	B/D	121	2.9	42
(010)	D/B	184	3.0	61

Table 4 : Ratios of theoretical and practical damping factors

Thus the effective area is independent of the actual area of the absorber* but depends only on the sound wavelength: the absorber receives sound energy from a much greater area of the incident wave-front than its own area would imply.

In the present case the absorber is not resonant, and furthermore the sound field in which it is situated is non-uniform. The theoretical approach which leads to Equation 35 is therefore not strictly applicable. There are nevertheless similarities between the present test conditions and the use of a resonant absorber, in that in both cases a localised site of absorption is surrounded by a large surface area for which the absorption is very much lower. It might therefore reasonably be expected that sound power flow into the absorber would take place from positions in the sound field other than those immediately in front of the absorber, as is implied by the theoretical considerations leading to Equation 1. This topic has been discussed in Section 3.3. As in the present case the absorbing patch is small compared with the sound wavelength in one dimension only, the distortion of the sound flow will only occur in planes normal to the long dimension (Fig. 9). Instead of deriving an effective area of absorber, as in Equation 35, therefore, an effective width (d_{eff}) may be assumed, such that

$$d_{eff} = (S_{eff})^{\frac{1}{2}} = \frac{\lambda}{2\sqrt{\pi}} \tag{36}$$

Table 5 shows the values of effective width involved in the present work.

The integration factors for a hypothetical absorbing patch having the measured long dimension but a short dimension equal to the effective width may now be calculated and new "theoretical" ratios

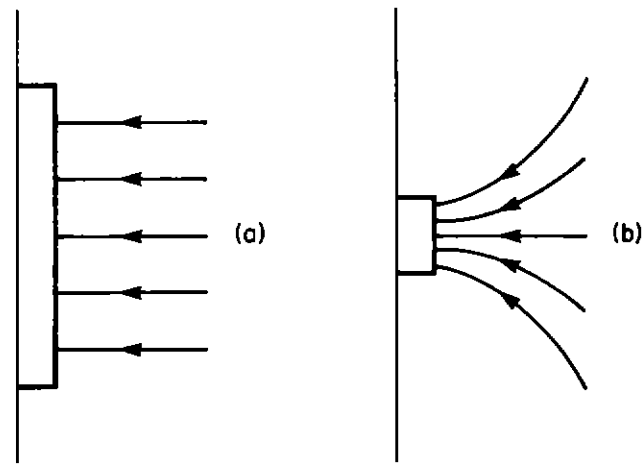

Fig. 9 – Illustration of sound power flow into an absorber having a dimension (a) comparable with wavelength, and (b) small compared with wavelength.
⟵ Sound power flow.

* Provided that this does not become too small: in such cases losses in the neck of the absorber increase and the absorption decreases.

Mode	*Frequency (Hz)*	*Wavelength (m)* ($c = 344.8\ ms^{-1}$)	*Effective width* (d_{eff}) *(from Equation 36)*
(100)	257	1.342	0.379
(010)	208	1.658	0·468

Table 5 : Calculation of effective width of absorbing patch

Mode	Absorbing patch positions used in obtaining ratio values	Damping factor ratios for conditions shown in Columns 1 and 2		Factor by which theoretical ratio exceeds practical ratio
		Theoretical (from equation 1)	From practical results (Table 3)	
(100)	B/D	4.4	2.9	1.5
(010)	D/B	4.4	3.0	1.5

Table 6 : Ratios of theoretical damping factors obtained using hypothetical absorbing patch with short dimension equal to effective width. Comparison with practical ratios also shown

of damping factor derived, following the procedure used to obtain the values in Column 3 of Table 4. Table 6 shows the results of this exercise. It can be seen that very much better agreement between theory and practice is shown when using "effective width" (Equation 36) as the short dimension of the absorbing patch, as compared with the use of the actual short dimension, to calculate the integration factors using Equation 1. Because of the rather uncertain theoretical justification for using the "effective width" concept, however, this greatly improved agreement between theory and practice must be treated with some reserve (see Sections 5.4 and 6).

It may be noted that if both dimensions of the absorbing patch are small compared with the sound wavelength, the above theory suggests that these dimensions should both be replaced by hypothetical "effective" values (or in other words, the area of the hypothetical absorber becomes S_{eff} as given by Equation 35). When both dimensions are comparable or much longer than a wavelength the actual patch dimensions should be used: between these two extremes there is a transition region which would require experimental investigation.

5.4. Tests using "shielding" absorbing patches

If an absorbing patch having a dimension small compared with the sound wavelength is surrounded by further absorbing material, the degree of convergence of sound power on to the original patch (see Section 5.3 and Fig. 9) will be reduced. This reduction in the degree of convergence of sound power should in turn reduce the effective area (S_{eff}, Equation 35) of an absorbing patch which is small (compared to the sound wavelength) in two dimensions, or the effective width (d_{eff}, Equation 36) of a patch which is small only in one dimension. The presence of "shielding absorbers" on each side of the type of absorbing strip used in the present tests should therefore reduce the disagreement between theoretical prediction and practical measurement noted in Section 5.2 (Table 4). Tests were carried out with the shielding absorbers taking the form of two absorbing patches of the same dimensions and construction as the test absorber, placed one on each side of this absorber (Fig. 10(a): see also Fig. 6). Reverberation times under these conditions were regarded as T_F in Equation 14. The "empty room" reverberation time T_E was obtained by removing the centre (test) absorber (Fig. 10(b)) while leaving the shielding absorbers in place. A third condition was also tested in which all three absorbers were present, but the test absorber was placed in an equivalent position in the room mode structure as compared with the first condition, but on the opposite wall of the enclosure (Fig. 10(c)). In this condition any effects due

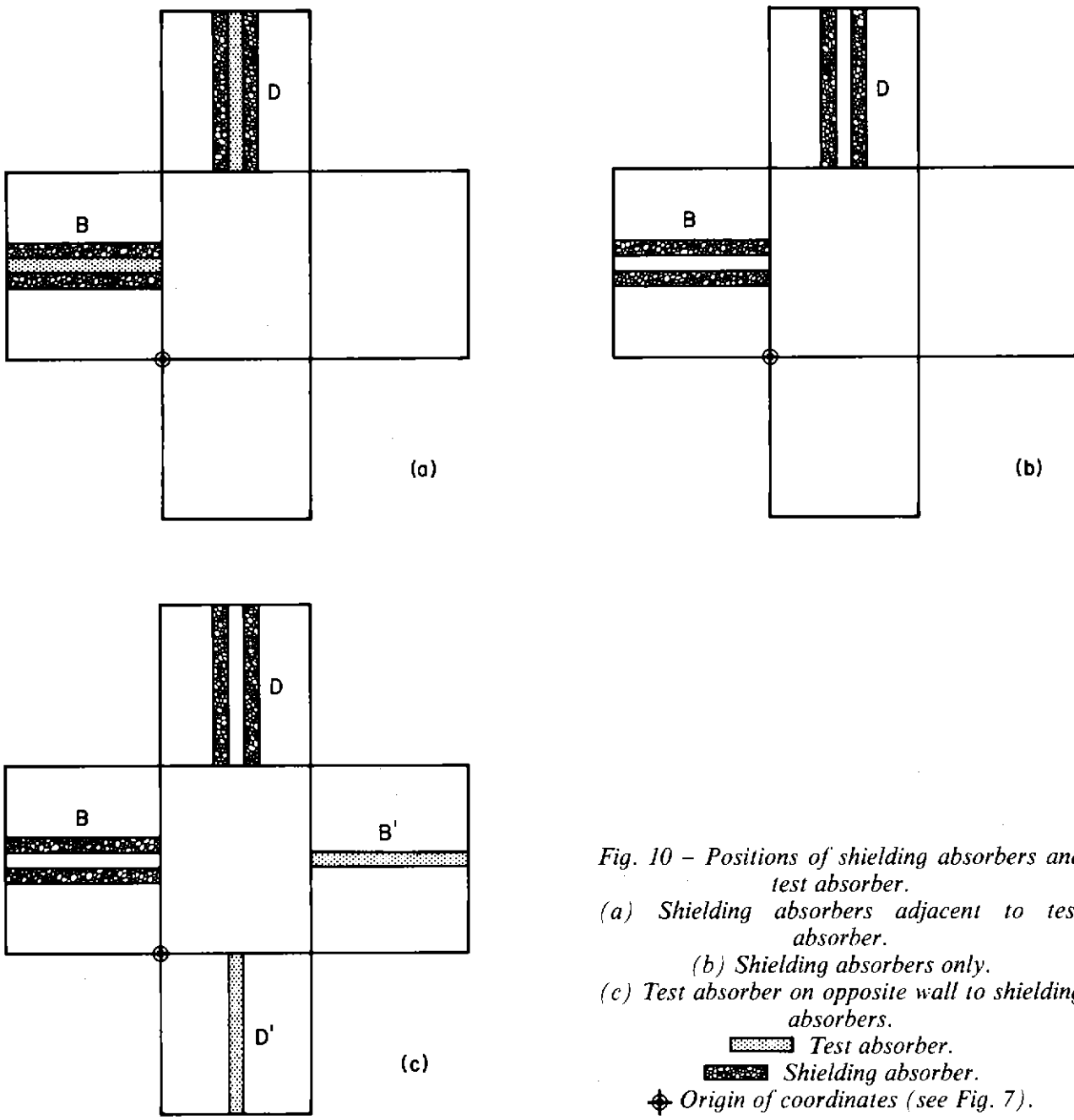

Fig. 10 – Positions of shielding absorbers and test absorber.
(a) Shielding absorbers adjacent to test absorber.
(b) Shielding absorbers only.
(c) Test absorber on opposite wall to shielding absorbers.
Test absorber.
Shielding absorber.
Origin of coordinates (see Fig. 7).

to the distortion of power flow by the shielding absorbers are still present, but the test absorber is not itself shielded. The results obtained from two independent sets of measurements of this type are shown in Table 7, the left-hand value in Columns 3 and 4 referring to one such set, and the right-hand value to the other. The scatter in the individual reverberation-time values, and the fact that the difference between the T_F and T_E values to be inserted into Equation 14 are much smaller than when only one absorbing patch is involved (see Sections 5.2 and 5.5), suggest that damping factors should be calculated from the individual measurements and averages then taken, rather than averages taken of the reverberation-times themselves. The damping factors shown in the last two columns of Table 7 have been derived in this way. Values corresponding to conditions where the test absorber was situated in a position of minimum potential energy density are shown in heavy type, in the same way as shown in Table 3. It can first be seen that in such conditions the damping factor is considerably reduced in value when the shielding absorbing patches are present on each side of the test absorber. By itself, this would appear to confirm the supposition that the sound power flow pattern is modified by the presence of the shielding absorbers, as discussed at the beginning of this Section. However, the damping factors remain much the same, whether the shielding absorbers are or are not present, when the absorbers are in a field

Position of shielding absorbing patches	Position of test absorbing patch	Measured reverberation time for indicated room mode		Value* of practical damping factor for indicated room mode	
		(100)	(010)	(100)	(010)
B	B	1.03 1.00	3.05 2.89	4.26	**0.17**
D	D	2.38 2.37	1.32 1.30	**0.27**	3.90
B	B′	0.96 1.04	2.53 2.54	4.51	**1.07**
D	D′	2.08 2.27	1.37 1.36	**0.89**	3.42
B	absent	1.43 1.38	3.20 2.95		
D	absent	2.40 2.56	2.06 1.85		

Table 7. Measured reverberation times and practical damping factors using "shielding" absorbing patches on each side of test absorbing patch

*multiply indicated values by 10^{-3}

of uniform sound potential energy density (light type in the last two columns of Table 7: also compare damping factors shown for absorber positions B′ and D′ in Table 7 with those for positions B and D in Table 3). This suggests that the sound power pattern is not affected by the presence of the shielding absorbers in this case. It would therefore appear that the nature of the sound power flow pattern changes, depending on whether an absorber is in a region of uniform or non-uniform potential energy density (or mean square sound pressure, in other words). Such a change would preclude using a simple "effective area" or "effective width" correction factor, as discussed in Section 5.3, since this factor itself would change with the nature of the sound field in the vicinity of the absorber.

5.5. Tests using absorbing patches not sealed to the walls of the test enclosure

It was noted in Section 4.2 that the test absorbers were sealed to the surface upon which they were mounted so that sound absorption could only occur at the exposed face of the absorber. Tests were however also conducted with this seal absent, there then being a gap of a few millimetres (on average) between the back of the absorber and the supporting surface. Table 8 shows average reverberation times

Absorbing patch position (see Table 2)	Measured reverberation time for indicated room mode and condition (sec)			
	(100)		(010)	
	sealed	not sealed	sealed	not sealed
A	2.09	3.14	2.74	3.65
B	2.18	3.07	4.03	3.89
C	2.71	3.11	3.83	4.09
D	3.81	3.02	2.50	3.55
Empty	6.35		5.78	

Table 8 : Measured reverberation times using one absorbing patch either sealed or not sealed to test enclosure wall

Patch position	Damping factors* and ratios for indicated conditions					
	(100)			(010)		
	sealed	unsealed	$\frac{\text{unsealed}}{\text{sealed}}$	sealed	unsealed	$\frac{\text{unsealed}}{\text{sealed}}$
A	5.00	2.51	0.51	2.99	1.57	0.52
B	4.69	2.62	0.56	**1.17**	**1.31**	**1.12**
C	3.29	2.55	0.78	1.37	1.11	0.81
D	**1.64**	**2.70**	**1.65**	3.53	1.69	0.48

Table 9 : Practical damping factors obtained using one absorbing patch either sealed or not sealed to test enclosure wall, with the ratio of corresponding factors for these two conditions also shown.

*multiply indicated values by 10^{-3}

obtained with the absorbers both sealed and not sealed to the surface. Table 9 shows the corresponding damping factors. (It may be noted that the data for the "sealed" absorbers has previously been given in Table 3, Section 5.2, and is repeated here for convenience). Table 9 also shows the ratios between the damping factors obtained under corresponding conditions with the absorbers sealed and not sealed. It may first be noted that the damping factors appear to be more mutually consistent when the absorbers are not sealed to the enclosure walls, compared with the values obtained under the "sealed" condition. For example, the same sound-field conditions (uniform and equal mean square sound pressure over the absorber surface) applies for the (100) mode for absorbers in positions A, B and C: the damping factors in these cases do not differ significantly from each other when the absorbers are not sealed to the walls, but do differ (as remarked in Section 5.2) when the "sealed" values are considered. It is possible that this reflects imperfections in the achieving of a good airtight seal between the absorber and its supporting surface, and illustrates the importance of tight control of the experimental conditions in an investigation of this type.

A more interesting relationship is revealed by examining the ratios between the damping factors obtained under corresponding conditions with the absorbers either sealed or not sealed to the walls of the test enclosure (Table 9, columns 4 and 7). It can be seen that this ratio is greater than unity when the absorber is placed at a position of minimum sound field potential energy density (heavy type in Table 9) but less than unity when the absorber is at a position of maximum potential energy density, or a position where a large part of the absorbing surface is not at a potential energy density minimum. Sound absorption apparently increases when the absorber is not sealed to the wall under the first of these conditions, but decreases under the second condition.

An explanation of the increase in sound absorption at a region of minimum potential energy density, when the absorber is not sealed to the supporting wall, may be found by considering the kinetic energy density of the sound field as well as the potential energy density. As discussed in Section 3.3, kinetic energy density is at a maximum where potential energy density is at a minimum. An absorber placed symmetrically at a potential energy density minimum (or mean square sound pressure minimum) will therefore experience a maximum of instantaneous sound pressure difference across its width (i.e. in the direction of sound propagation in the standing-wave pattern within the enclosure). This pressure difference will tend to drive air through the small gap behind the absorber and frictional losses in this gap will introduce an additional component of absorption which is not present when the gap is sealed.

At a region of potential energy density (or mean square sound pressure) maximum the kinetic energy density is zero and no differential instantaneous sound pressure exists across the width of the absorber. There will therefore be no tendency for air to be driven through the gap behind the absorber

and no additional component of absorption will be introduced. In fact, a porous absorber such as was used during the tests described in this Report is rendered less effective under these conditions if both its front and rear surfaces are exposed to the ambient sound field: a sound pressure "neutral plane" is formed half way through the depth of the absorber, and the effective halving in the thickness of the absorber is not compensated by the doubling in absorbing surface area. Unsealing the absorber from the wall would expose its rear surface to the ambient sound field and this could account for the observed decrease in absorption.

In general, it appears that the absorbing patch must be considered sensitive to both kinetic and potential sound energy density and the relationship between amount of absorption and position in the room mode structure depends on the balance between these two factors. Predominance of the potential energy density component (e.g. with the absorber sealed to the wall) will give rise to a reduction in absorption on change of absorber position from a sound pressure maximum to a sound pressure minimum, while predominance of the kinetic energy density component (e.g. with the absorber not sealed to the wall) will give rise to an increase of absorption under these conditions. An absorber which happened to have equal sensitivity to potential and kinetic energy density would show no change of absorption under these conditions. Even when the absorber is sealed to the walls of the enclosure it may show some sensitivity to kinetic energy density, as the instantaneous sound pressure difference across the surface may introduce a component of air movement through the absorber in a direction parallel to the surface of the absorber: this could at least in part account for the differences between theoretical predictions and practical measurements discussed in Section 5.2.

6. Discussion

The theoretical relationship between absorber size and position in relation to the standing-wave (room mode) pattern on the one hand, and the amount of absorption on the other hand, has been shown to apply when the absorber is sensitive only to sound potential energy density and not to kinetic energy density (or in other words, on the instantaneous sound-pressure gradient across it). This condition is fulfilled if the absorbing material is "locally reacting", so that absorption at one elementary area on its surface depends only on the sound pressure immediately adjacent to this area and is independent of the conditions applying at other regions of the absorber. Porous materials are usually regarded as locally reacting, and this consideration governed the choice of material ("high-density" mineral wool) used to construct the test absorbers used in this investigation. In spite of this precaution, one of the reasons for the discrepancy between theory and practice which has been observed in this work appears to be the sensitivity of the material to sound pressure gradient (see Section 5.5). Mineral wool is widely used as absorbing material and it is revealing to find that it (or other similarly-constructed porous materials) cannot strictly be regarded as locally-reacting. It would be instructive to repeat the tests using an absorber containing many small channels normal to its surface, with no cross-connections between these channels: this would perhaps approach the "locally-reacting" condition more closely. The effect of permitting a small unsealed air-space to remain behind the absorber is also noteworthy, particularly as absorbers are in practice frequently mounted with an air-space behind them to clear electrical conduit and other pipework that may be fixed to the studio wall. However, the dimensions of an air-gap clearly influence the amount of absorption that it will introduce and the magnitude of the effects observed in the present work cannot necessarily be regarded as typical. It may be noted that the observed effect of introducing an unsealed air-gap was perhaps exaggerated by the rather low absorption of the test absorber itself: the average damping coefficient of about 2.5×10^{-3} found during the tests corresponds (Equation 34) to a conventional absorption coefficient of 0.2. The principal interest in this aspect of the work lies in the insight that it gives into the sound absorption mechanism, although it serves as a useful reminder of the practical effects that may be introduced by air gaps behind absorbers.

Earlier work which examined the influence of room mode structure on sound absorption[1] was concerned principally with effects which occurred in a rectangular room having all walls of uniform specific acoustic impedance. In this work, it was assumed that sound absorption at a surface was proportional to the mean square pressure (or in other words to the potential energy density). This work showed[1a,1c] that, if $\bar{\alpha}$ is the absorption coefficient of the surface in the presence of a uniform mean square sound pressure (and therefore energy density) distribution across it, then under certain simplifying conditions the effective absorption coefficients in the presence of only axial, tangential or

oblique room modes ($\bar{\alpha}_{ax(p)}$, $\bar{\alpha}_{ta(p)}$ and $\bar{\alpha}_{ob(p)}$ respectively) are given by

$$\begin{aligned} \bar{\alpha}_{ax(p)} &= \tfrac{2}{3}\bar{\alpha} \\ \bar{\alpha}_{ta(p)} &= \tfrac{5}{6}\bar{\alpha} \\ \bar{\alpha}_{ob(p)} &= \bar{\alpha} \end{aligned} \tag{37}$$

In Equations 37 the subscript p indicates, as in Section 3 of this Report, sensitivity of the absorbing material to potential energy density only. From these relationships a prediction could be made[1d] of the ratio (R_T) of the two values of effective absorption coefficient found when the complete surfaces of two rooms of different dimensions were treated with the same material: this prediction also involved a knowledge of the proportions of the three classes of room mode occurring in each room for each frequency band under consideration. A similar analysis can be made on the assumption that only kinetic energy density is involved in the mechanism of absorption (in other words, that the absorbing medium is sensitive to sound pressure gradient across its surface but not to sound pressure at particular points on it). For a surface of the room where the mean square sound pressure varies according to a raised cosine law either in one direction or in two orthogonal directions, the effect of integrating the energy density over the surface is the same whether potential or kinetic energy density is concerned. In the cases of tangential and oblique room modes, the energy density distribution across all the room surfaces corresponds to one or other of these categories. Thus, using (again as in Section 3) the subscript k to denote sensitivity to kinetic energy density only, the relationships between $\bar{\alpha}$ on the one hand, and $\bar{\alpha}_{ta(k)}$ or $\bar{\alpha}_{ob(k)}$ on the other hand, are the same as the corresponding relationships in Equations 37. For axial room modes, however, the kinetic energy density at the two walls normal to the direction of sound propagation in the room is zero, in contrast to the value of potential energy density which is at a maximum over these surfaces. This has the effect of halving the value of $\bar{\alpha}_{ax(k)}$ relative to the corresponding value of $\bar{\alpha}_{ax(p)}$. Thus

$$\begin{aligned} \bar{\alpha}_{ax_{(k)}} &= \tfrac{1}{3}\bar{\alpha} \\ \bar{\alpha}_{ta_{(k)}} &= \tfrac{5}{6}\bar{\alpha} \\ \bar{\alpha}_{ob_{(k)}} &= \bar{\alpha} \end{aligned} \tag{38}$$

In practice it is likely, as has been indicated in the present work, that an absorber will be sensitive to both potential and kinetic energy density. In such cases a value of $\bar{\alpha}_{ax}$ lying between the extreme values shown in Equations 37 and 38 will be obtained. For example, if these sensitivities are equal,

$$\begin{aligned} \bar{\alpha}_{ax} &= \tfrac{1}{2}\bar{\alpha} \\ \bar{\alpha}_{ta} &= \tfrac{5}{6}\bar{\alpha} \\ \bar{\alpha}_{ob} &= \bar{\alpha} \end{aligned} \tag{39}$$

These values can be used, instead of those given in Equations 37, in deriving the value of the ratio R_T discussed above. Fig. 11 (which is based on Fig. 9 of Reference 1) shows the predicted values of R_T under conditions corresponding to Equations 37 and 39, compared with the practical results discussed in Reference 1. It can be seen that the principal differences in these predicted values occur as expected at low frequencies, where the proportion of axial room modes in the two rooms (particularly the smaller one) is greater, and also that, in general, sensitivity to kinetic as well as potential energy density leads to a greater change in overall average absorption coefficient between one treated room and another of different size.

The abstraction of energy from parts of the sound field not immediately adjacent to the absorber, when the absorber has a dimension small compared with the sound wavelength (Section 5.3), appears to represent an important reason for the observed differences between theoretical prediction and practical measurement of absorption. The incorporation of this easily-calculated factor into the theoretical model of sound absorption would, at first sight, provide a convenient starting-point for further comparisons between theory and practice, involving perhaps a number of absorbing patches (rather than only one, as in the present investigation) and enclosures of different sizes. There are however a number of reasons why caution should be exercised in the adoption of this line of approach. In the first

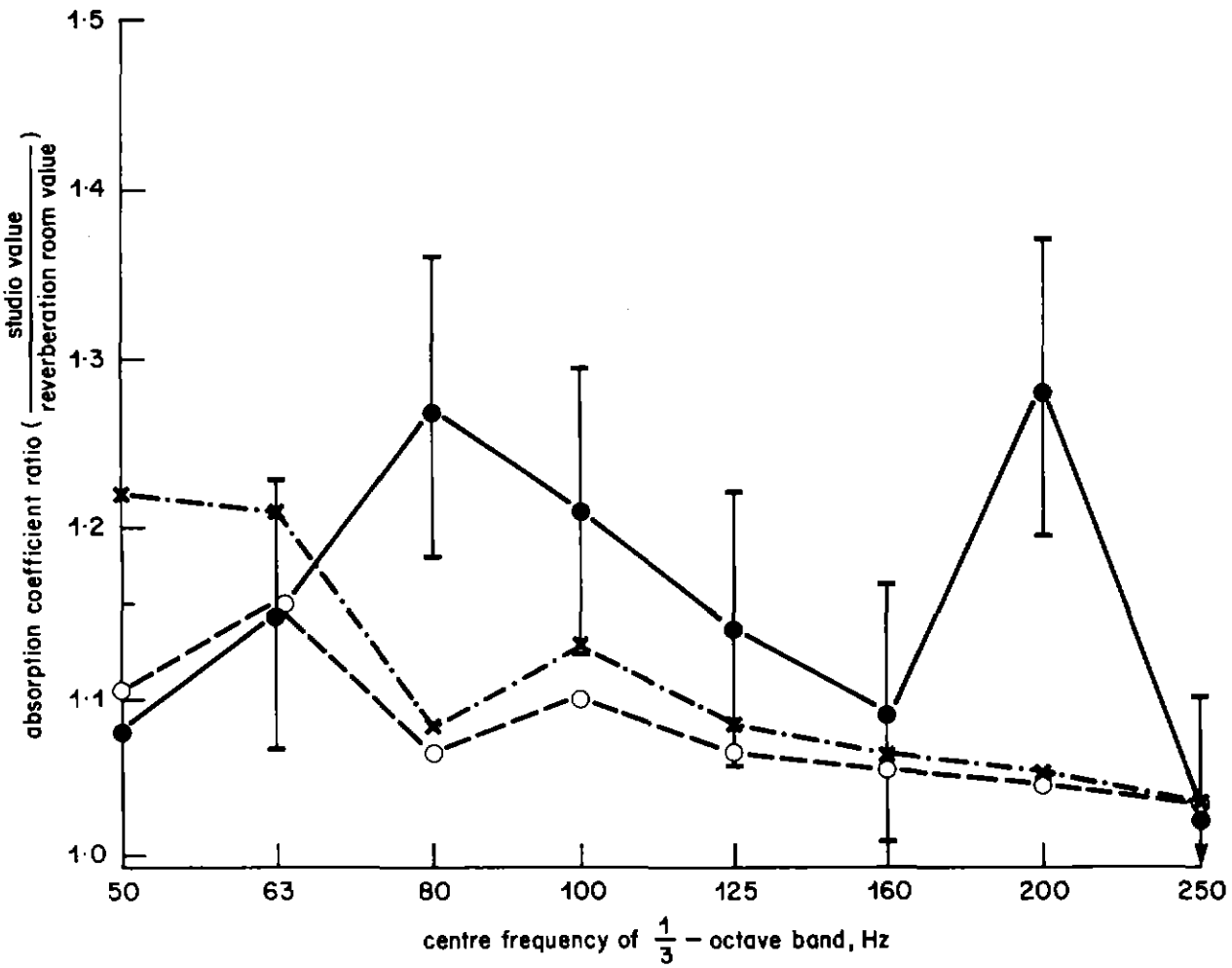

Fig. 11 – Practical and theoretical ratios of the absorption coefficient of a particular type of absorber, when placed in two rooms of different sizes.

Practical measurements with confidence limits.

Absorber assumed sensitive to potential energy density only. } *Theoretical predictions*

Absorber assumed equally sensitive to potential and kinetic energy density. } *predictions*

place the concept of "effective area" or "effective width" only applies when the appropriate absorber dimension is small compared with the sound wavelength: there is no simple method of scaling this effective dimension as the actual absorber dimension is increased to become, eventually, the same order as wavelength. Secondly, there is evidence (Section 5.4) that the effective dimension of a sound absorber changes with the nature of the sound-field in which it is placed. And, thirdly, the abstraction of energy from parts of the sound field not immediately adjacent to the absorber has been shown not to be the only reason for the discrepancy between theory and practice: on the evidence at present available it is not possible to ascribe greater or less importance to either this factor or the sensitivity to sound pressure gradient, as previously discussed.

A property of a locally-reacting surface is that its specific acoustic impedance is independent of the direction of the incident sound.[5] It is this property that makes the theoretical approach outlined in Section 2 applicable only to locally-reacting surfaces. The behaviour of the lid of the test enclosure (see Section 5.1) in the presence of different room modes is illustrative of a non-locally-reacting surface whose specific acoustic impedance changes markedly with change of room mode (and therefore incident sound direction). As might be expected, the theoretical approach does not describe the change in absorption observed in practice in these circumstances. Many absorbers used in practice rely on panel excitation rather than, or in addition to, sound absorption at porous surfaces, and in these cases the formal theoretical approach is likely to be misleading. Nevertheless the factors which have been discussed in this Report enable an appreciation of the mechanisms of sound absorption to be obtained,

and give at least a qualitative insight into the relationships between the amount of absorption obtained and the size and disposition of the absorbing surfaces relative to the standing-wave pattern or "room mode structure" in the enclosure.

7. Conclusions

Three factors have been identified which account for the differences between the practical amounts of sound absorption obtained when an absorber is exposed to different standing-wave pattern configurations on the one hand, and corresponding theoretical predictions of change of absorption, based on the treatment of the subject by Dowell,[2] on the other hand. These are:

1. The dependence of the degree of absorber excitation on the standing-wave pattern in which it is placed.
2. The dependence of the amount of absorption on both the potential and kinetic energy densities of the sound field in the vicinity of the absorber.
3. The flow of energy into the absorber from regions of the sound field that are not immediately adjacent to it.

The first of these factors applies particularly to panel absorbers having dimensions comparable with the sound wavelength. It implies that the specific acoustic impedance of the absorber depends on the standing-wave pattern to which it is exposed: the theoretical prediction, on the other hand, assumes that this quantity remains constant. The theoretical relationship also implies a direct relationship between amount of absorption and the distribution of mean square sound pressure (or potential energy density) over the absorbing surface. Both the second and third of the factors listed above violate this assumption; the second in that sound pressure-difference across the absorber, as well as sound pressure at points on its surface, contributes to the total amount of absorption that takes place, and the third in that sound pressure in parts of the sound field not immediately adjacent to the absorber have to be taken into account. The second factor would not apply in cases where the absorbing surface is strictly "locally-reacting", when absorption at a small area depends only on the sound pressure at that area. However, it appears that practical absorbers constructed from materials such as mineral wool do not strictly conform to this criterion. The third factor applies particularly when at least one dimension of the absorber is small compared with the sound wavelength. In such cases it may be possible to assign "effective" dimensions to the absorber to take account of the enhanced energy flow into it.

The present work does not indicate the relative importance of the factors, described above, which contribute to the discrepancy between theory and practice in the prediction of change of absorption with room mode structure. This relative importance is in fact likely to differ between absorbers of different types and geometries. On present evidence it does not appear possible to envisage a purely theoretical general method of carrying out such a prediction. However, it may still be practicable to investigate the behaviour of individual types of absorber experimentally, and derive relationships which would enable their absorption to be predicted in different environments with a greater degree of certainty than can at present be achieved using existing standard techniques.

8. References

1. TAYLOR, E.W. A preliminary study of the influence of room mode structure on sound absorption. BBC Research Department Report No. 1983/4.
   1a. Ibid., Appendix. 1c. Ibid., Section 4.
   1b. Ibid., Equation 21. 1d. Ibid., Equation 41.

2. DOWELL, E.H. Reverberation time, absorption and impedance. J. Acoustic Soc. Am. *64*, 1, (July 1978) pp. 181–191.

3. BERANEK, L.L. Acoustics. McGraw-Hill Publishing Co., Ltd., London, 1954. pp. 40–42.

4. WOOD, A.B. A textbook of sound: pp. 373–376. G. Bell and Sons Ltd., London, 1930.

5. KUTTRUFF, H. Room acoustics. Applied Science Publishers, Ltd., London, 1973. p. 23.

Printed by BBC RESEARCH DEPARTMENT, Kingswood Warren, Tadworth, Surrey, KT20 6NP